Ultrafast Dynamics of Isolated Model Photoactive Yellow Protein Chromophores: "Chemical Perturbation Theory" in the Laboratory

Mikas Vengris,*,† Delmar S. Larsen,*,†,§ Michael A. van der Horst,‡ Olaf F. A. Larsen,† Klaas J. Hellingwerf,‡ and Rienk van Grondelle†

Faculty of Sciences, Vrije Universiteit Amsterdam, De Boelelaan 1081, 1081 HV Amsterdam, The Netherlands, and Department of Microbiology, Swammerdam Institute for Life Sciences, University of Amsterdam, Nieuwe Achtergracht 166, 1018 WS Amsterdam, The Netherlands

Received: September 17, 2004; In Final Form: December 6, 2004

Pump−probe and pump−dump probe experiments have been performed on several isolated model chromophores of the photoactive yellow protein (PYP). The observed transient absorption spectra are discussed in terms of the spectral signatures ascribed to solvation, excited-state twisting, and vibrational relaxation. It is observed that the protonation state has a profound effect on the excited-state lifetime of *p*-coumaric acid. Pigments with ester groups on the coumaryl tail end and charged phenolic moieties show dynamics that are significantly different from those of other pigments. Here, an unrelaxed ground-state intermediate could be observed in pump−probe signals. A similar intermediate could be identified in the sinapinic acid and in isomerization-locked chromophores by means of pump−dump probe spectroscopy; however, in these compounds it is less pronounced and could be due to ground-state solvation and/or vibrational relaxation. Because of strong protonation-state dependencies and the effect of electron donor groups, it is argued that charge redistribution upon excitation determines the twisting reaction pathway, possibly through interaction with the environment. It is suggested that the same pathway may be responsible for the initiation of the photocycle in native PYP.

1. Introduction

Light-induced reactions, especially those that include structural changes in molecules, have long been of interest for scientists. Understanding these reactions represents not only a scientific challenge but also has significant relevance for industry and biology. The molecules that undergo photoinduced reactions have potential applications in such areas as optical memory, optoelectronics, solar cells, molecular switches, etc.[1−3] Studying these molecules relates to a multitude of condensed-phase processes of fundamental importance, including charge redistribution, solvation, *trans*−*cis* isomerization, and inter- and intramolecular vibrational relaxation. Important processes of life, including human vision,[4] bacterial photosynthesis,[5] plant phototropism,[6] and bacterial phototaxis[7] are also initiated by these reactions.

To be successful, the rates of photoinduced excited state reactions must compete effectively with the lifetime of electronic excitation in these molecules (usually of the order of several ns for singlet excited states), which puts these reactions in the realm of ultrafast laser spectroscopy. Numerous ultrafast studies on "classical" isomerizing molecules such as *trans*-stilbene,[8] auramine,[9] and the protonated Schiff base[10] containing polyenes have revealed that the rates of these reactions are in the (sub)-picosecond time domain. The answer to the question as to how the reactions are actually proceeding is encrypted in the excited-state potential-energy surfaces (PESs) of these molecules, which ultimately define the driving force for the reaction. The solvent environment also plays a key part in determining the course of the reaction. In biological systems, an even more important role is played by the protein environment because the protein reacts to the structural change of the pigment and performs its relevant biological function (e.g., in bacteriorhodopsin, a proton is transferred across the membrane, and photoactive yellow protein (PYP) changes its conformation to alter its interaction(s) with the signaling partner).

One of the better characterized proteins with a biological function based on an isomerization photoreaction of an intrinsically bound chromophore, is the PYP. Because of its small size and excellent stability, it has become a model system for studying biological light-induced signal transduction.[7] PYP is a small (14 kDa) water-soluble protein belonging to the PAS domain family and was originally discovered in the photosynthetic bacterium *Halorhodospira halophila*,[11] where it initiates a negative phototactic response to blue-light illumination.[12] A significant amount of research on this protein was triggered by the resolution of its stationary (both room temperature and cryotrapped)[13] and time-resolved X-ray structures.[14−16] These structures confirmed the earlier assertion that PYP contained a *p*-coumaric acid chromophore (pCA)[17] that is covalently bound to the protein backbone via a thioester linkage to the cysteine-69 residue. This pigment is buried inside a protein pocket that protects it from the solvent environment; in the dark-adapted ground state, its phenolic moiety is deprotonated, and the negative charge is stabilized by the network of hydrogen bonds with neighboring amino acid residues. Upon blue-light excitation of the pCA pigment, a complex photocycle is initiated that exhibits a dynamic sequence of intermediates occurring on multiple time scales from tens of femtoseconds to seconds,[7]

* Authors to whom correspondence may be addressed. E-mail: mikasv@nat.vu.nl (M.V.); dlarsen@usc.edu (D.S.L.).
† Vrije Universiteit Amsterdam.
‡ University of Amsterdam.
§ Current address: Department of Chemistry, University of Southern California, Los Angeles, CA 90089.

10.1021/jp045763d CCC: $30.25
Published on Web 02/15/2005

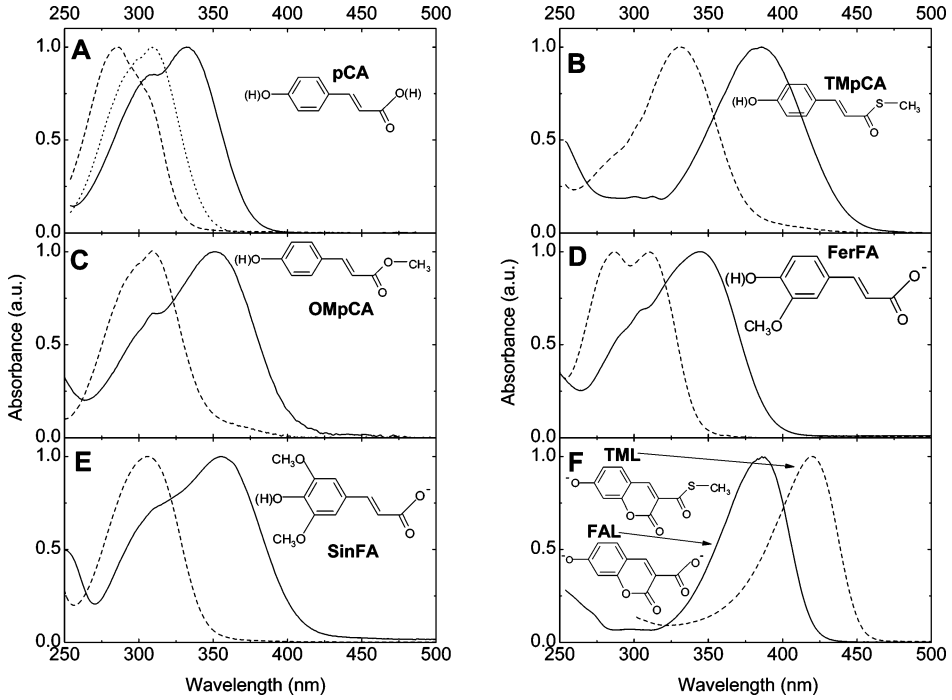

Figure 1. Absorption spectra and structural formulas of the PYP model chromophores investigated in this study. In all panels, except panel F, the solid, dashed, and dotted lines represent the spectrum measured at Ph = 10.5, 7, and 2, respectively. (A) pCA; (B) TMpCA; (C) OMpCA; (D) FerFA; (E) SinFA. (F) FAL is the solid line, while thiomethyl locked TML is demarked by a dashed line.

including a *trans*−*cis* isomerization and protonation of the pCA chromophore and a partial unfolding of the protein.[18,19] The partially unfolded form of PYP is the presumed signaling state responsible for biochemical signal transduction.[20] The original configuration of the protein and the chromophore is recovered on a time scale of 0.1−1 s.

Recently, a number of spectroscopic ultrafast studies have focused on investigating the initial dynamics of PYP.[21−25] Furthermore, mutants with genetically engineered changes in the chromophore-binding pocket, along with hybrid proteins containing non-native pigments, have been examined.[21−23,25−30] Changing the amino acid residues in the protein pocket consistently appears to slow the excited-state decay,[27] whereas the incorporation of a nonisomerizing pigment analogue into the protein has been shown to completely block the signaling-state formation.[7,31] Some mutations, and especially a combination of a mutation plus a replacement of the native pigment, resulted in a dramatic change in the color of the protein.[32] Some of the key questions addressed in these studies was to what extent the photoinduced dynamics in PYP is dictated by the dynamics inherent to the chromophore and how this dynamics is tuned by the protein environment, or by the interactions between the two. Previously, several potential model PYP chromophores have been investigated in solution with ultrafast spectroscopic techniques.[33−36] In model chromophores containing a thioester moiety, an unrelaxed ground-state intermediate has been observed that was ascribed to a twisted conformation of the chromophore, which subsequently returned back into the equilibrated ground-state structure. Similar spectroscopic features have also been observed in the native PYP system,[37] suggesting that the study of specific isolated chromophores can be useful for exploring the chromophore dynamics in PYP.[21,25,34,37]

In this paper, we present a systematic study of the dynamics of several PYP model compounds, with an emphasis on identifying the dynamical effects arising from changing the structure, pH, or excitation wavelength. Dispersed pump−probe (PP) and pump−dump probe (PDP) data on the seven different pigments (Figure 1) in aqueous solution are contrasted and compared. While all the studied chromophores share the same carbon backbone, which is identical to the native PYP chromophore,[38] they differ in the nature of their substituents and protonation state. The thiomethyl ester derivatives of pCA (TMpCA) explore the role of the thioester linkage, which is also present in the PYP protein (provided by the Cys69 residue), on the ensuing dynamics, and these observations are contrasted with the oxy-methyl-pCA (OMpCA) chromophores, where this ester linkage contains the lighter oxygen atom instead. Ferulic (FerFA) and sinapinic (SinFA) acids contain one and two methoxy groups, respectively, attached to the phenolic ring of the pigment, which may sterically hinder the twisting reaction and/or may function as electron-donating groups which alter the charge distribution in the conjugated system and affect the charge-transfer character of the electronic transition. The data collected for these free-twisting chromophores are contrasted with locked chromophores, where the possibility of twisting/isomerization is prevented by the introduction of additional covalent bonds. The free-acid-locked (FAL) and the thiomethyl-locked (TML) derivatives are useful to identify observed dynamical features that originate from processes other than twisting, such as solvation and vibrational relaxation.

Because the chromophore binding pocket in PYP is tuned to generate a high pH (∼9.8), experiments on the pigments were performed at different pH values to investigate the effect of protonation on the light-induced dynamics. Thus, by collecting these data on a variety of chromophores and under various conditions, a sort of "chemical perturbation theory" has been applied in the laboratory to explore the intrinsic dynamics of the PYP chromophore.

2. Experimental Section

2.1. Samples. The pCA, SinFA, and FerFA chromophores were purchased from Sigma-Aldrich, while FAL was purchased from Molecular Probes; these pigments were used without

further purification. The thiomethyl derivatives were synthesized from their respective free acids (via the 1,1-carbonyldiimidazole intermediate) and sodium thiomethoxide (Acros Organics, Geel, Belgium). Equimolar amounts were mixed and allowed to react overnight at room temperature. The chromophores were purified with a silica gel column by washing with two column volumes of petroleum ether and then eluted with a 1:1 (v/v) ethyl acetate/petroleum ether mixture. For the synthesis of OMpCA (methyl-coumarate or 4-hydroxycinnamic methylester), 1 mmol of 4-hydroxy-cinnamic acid was dissolved in 10 mL of methanol, and a catalytic amount of concentrated sulfuric acid was added (a few drops). The reaction mixture was stirred overnight at room temperature and evaporated under reduced pressure, and the product was further purified by recrystallization from a petroleum ether−ethyl acetate mixture.

The identity and purity of the synthesized compounds was confirmed with NMR and mass spectrometry. The samples were buffered with 50 mM CAPS buffer at a pH of 10.5 or 50 mM phosphate buffer for pH = 7 and 2 and were prepared with optical densities (OD) between 0.5 and 0.7 per mm at the absorption maximum (Figure 1).

2.2. Ultrafast Setup. The PP setup has been described in detail earlier[36,39] and has been modified to generate excitation light in the near-UV region. The basis of the system is a 1-kHz amplified Ti:sapphire system (BMI α) delivering 400-μJ, 60-fs, and 790-nm pulses. The dispersed PP experiments presented were performed at two excitation wavelengths: 395 nm and in the near-UV region (between 310 and 350 nm). The 395-nm pump pulses were generated by frequency doubling a portion of the amplified 790-nm light in a 0.5 mm thick BBO crystal, while the UV pump pulses were generated by mixing the 475−625 nm output of a home-built 395-nm-pumped noncollinear optical parametric amplifier (NOPA) with the fundamental in the 0.4 mm thick BBO crystal. For three-pulse PDP experiments, the 505-nm beam from the NOPA was introduced as a dump pulse.[37] The white-light continuum, used as the broad-band probe pulse, was produced by focusing a weak 790-nm beam into a slowly translating CaF_2 crystal. The delay between pump and probe pulses was varied using motorized, computer-controlled translation stages (Newport). The samples were pumped through a rapidly translating 1-mm quartz flow cell. The polarization of the pump (and dump) pulse was kept at magic angle (54.7°) with respect to the probe pulse. The group velocity dispersion (GVD) of the white light was estimated from the measurement of the cross-phase modulation artifact in water and was further refined in the global fitting procedure, and the data were corrected for GVD prior to presentation.

The collected data constitute a three-dimensional surface with ca. 250 wavelength points and ca. 100 time points. In the case of PDP experiments, it actually consists of three surfaces, corresponding to PP (pump pulse on, dump pulse off), DP (pump pulse off, dump pulse on), and PDP (both pump and dump pulses are on) data. The wavelength resolution of the data is ca. 1 nm, and time resolution is ∼130 fs with 395-nm excitation and ∼370 fs with UV excitation respectively, both with an average noise level of ∼1 mOD.

2.3. Data Analysis. The PP data was fitted globally using an evolutionary model (i.e., $A \xrightarrow{\tau_1} B \xrightarrow{\tau_2} C \xrightarrow{\tau_3} ...$),[40,41] which reduces the often unwieldy time-resolved and wavelength-resolved data to a set of a small number of spectra (typically around five), which evolve into each other with consecutively decreasing lifetimes of τ_1, τ_2, etc. Time evolution of the spectrum can thus be described in a concise parametric manner; however, the obtained species-associated difference spectra (SADS) do not necessarily represent the real spectra of the excited-, ground-, and product-state species that occur in the experiment.[41,42] As opposed to the ubiquitous application of fitting measured data to a "sum of exponential decays," which essentially is a parallel model, the estimated SADS resulting from a sequential model resemble the real PP spectra measured at certain delay times. Thus, sequential SADS are often more intuitive to interpret than the raw data directly. For a more detailed discussion about the applicability of various models and the interpretation of the results of global and target analysis the reader is referred to references.[41−43]

In all the fits presented here, a component shorter than the time resolution of the instrument (lifetime ca. 100 fs for 395 nm excitation and ca. 250 fs for 310−350 nm excitation) was introduced to adequately describe the data. The SADS corresponding to this component, however, is significantly contaminated by the cross-phase modulation artifact between the pump and probe pulses[43,44] and has been omitted from the presented global analysis figures.

3. Results

The experimental results section is organized in the following manner: first, the raw PP data of the investigated pigments are discussed. Because of space considerations, we only discuss the data explicitly for two systems: pCA at pH 10.5 and SinFA at pH 10.5, and for the other pigments, only the raw kinetic traces measured at the maximum of the stimulated emission (SE) band are presented. Additionally to the raw data, we present the corresponding SADS resulting from the sequential global analysis fit to the data, which illustrates the spectral aspects of the ensuing dynamics. Next, the results of wavelength-dependent PP experiments and finally the PDP data on SinFA and locked chromophores are presented.

3.1. Transient Absorption. The pCA and SinFA PP datasets measured at pH 10.5 are compared in Figure 2. The excitation wavelength was 330 nm for pCA and 395 nm for SinFA. Every point in the kinetic traces (parts A and C of Figure 2) is taken from a measured time-gated spectrum, several of which at different probe delay times are shown in parts B and D of Figure 2. The spectral features of both compounds are qualitatively similar: a positive induced absorption (IA) band is observed at high probe energies (ca. 360 nm for pCA and 400 nm for SinFA), which overlaps the ground-state absorption, while a negative SE band peaks at lower probe energies (430 nm for pCA and 485 nm for SinFA). For both chromophores, the IA obscures the expected ground-state bleach (parts A and E of Figure 1). The time-gated spectra in parts B and D of Figure 2 exhibit a dynamic red-shifting of the SE on the <2-ps time scale. From the comparison of the spectra obtained at 500 fs and 2 ps for pCA (Figure 2A), a clear decay of the IA band is observed that is not correlated with a loss in the SE band. However, on the longer time scales (> 2 ps), the decay of the SE and IA bands is identical, indicating that this IA is due to the excited-state absorption (ESA). In both samples, the kinetic traces around the zero crossing point of the spectrum (the spectral region, where ΔOD = 0 at different delay times, see the spectra in parts B and D of Figure 2) show a behavior different from either the SE or ESA bands; initially the signal is negative, but after 1 ps, it crosses zero, reaches the positive maximum at around 3 ps, and then decays to zero. At these wavelengths that correspond to the zero-crossing point of the spectrum, the kinetic traces are very sensitive to spectral shifts and the appearance of new bands; the observed behavior is indicative of a shifting SE band or a growth and decay of a product absorption.

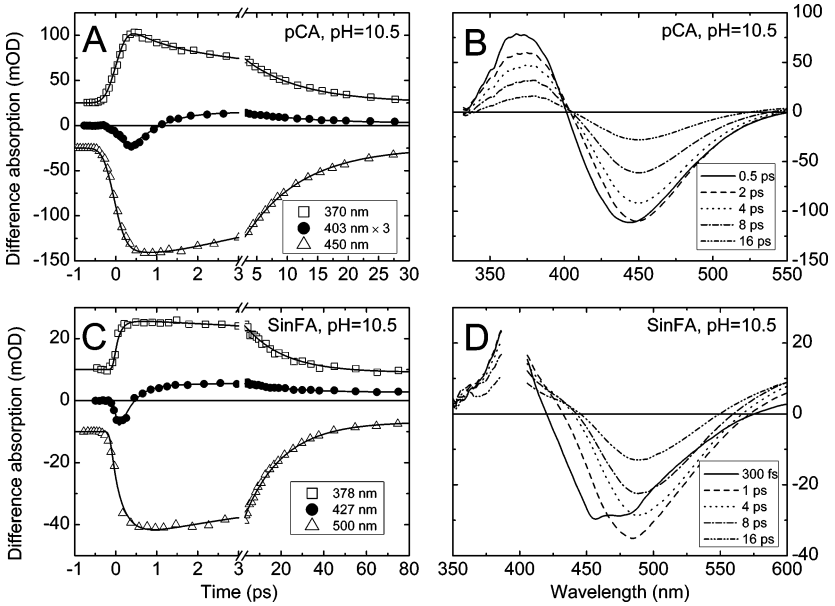

Figure 2. Dispersion-corrected PP data on pCA (A and B) and SinFA (C and D) at pH = 10.5. (A and C) Kinetic traces at the ESA band (squares), around the zero-crossing point (circles), and SE band (triangles). The traces at the zero crossing point have been multiplied 3-fold, and the traces at ESA and SE bands have been offset by 25 and −25 mOD (10 and −10 mOD for SinFA), respectively. The probe wavelengths for the traces are shown in the legends. The solid lines show the global analysis fit through the data. Note the break in the time axis. (B and D) Time-gated spectra measured at the probe delay times shown in the legends. In SinFA data (D), the spectral region around 395 nm was corrupted by the scattering of the pump light and is not shown.

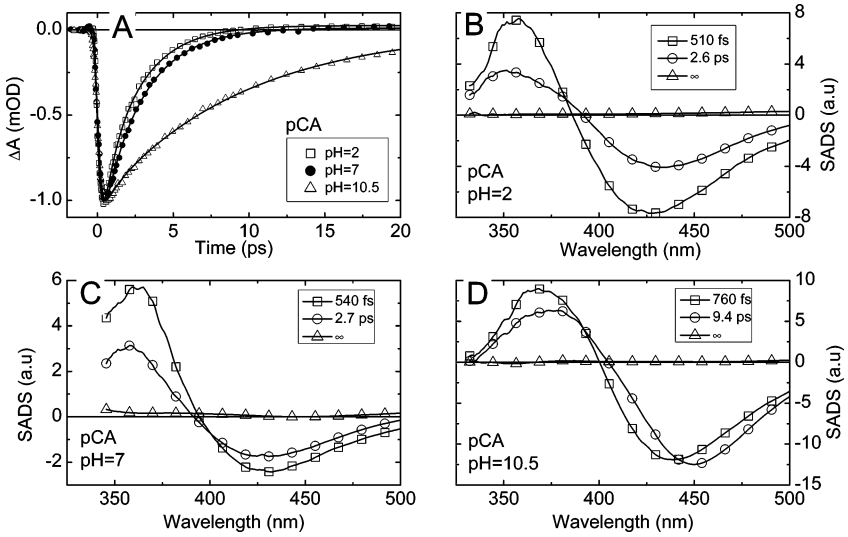

Figure 3. (A) Kinetic traces measured at the SE band of pCA at pH = 2 (open squares), 7 (filled circles), and 10.5 (open triangles). The excitation wavelength was 310 nm, and the probe wavelength for the shown traces was 430 nm. Solid lines show the global analysis fit to the data. (B, C, and D) SADS resulting from the sequential model fit to the data measured on pCA at pH = 2, 7, and 10.5, respectively. The estimated time constants for the spectral evolution are shown in the legends.

The pH dependence of the spectra and kinetics for pCA is presented in Figure 3. The decay of the SE band at pH = 2 and 7 is nearly pH independent (slightly faster at pH = 2). However, at pH = 10.5, a significant decrease in the decay rate is observed (Figure 3A, open triangles). At pH = 2 and 7, essentially all the transient absorption signal decays on a 2.6-ps time scale, whereas at pH = 10.5 the decay takes 9.4 ps (parts B, C, and D of Figure 3). For all three pHs, the SADS exhibit a faster initial decay in the IA band than in SE band as observed in Figure 2B. A slight red-shift of the SE is observed with a time constant of ca. 500 fs at pH = 2 and 10.5; however, it is nearly absent at pH = 7. At all pH values, a nondecaying component is also observed; it has a near-zero amplitude and exhibits only an induced absorption.

OMpCA and TMpCA exhibit much richer dynamics than pCA. The dispersed PP data on these compounds at pH = 7 (excitation wavelength 310 nm) and 10.5 (excitation wavelength 395 nm) are shown in Figure 4. The OMpCA data at pH = 7 (Figure 4C) closely resemble those obtained with pCA (Figure 3): a 12-nm red-shift of SE is observed on a 570-fs time scale along with a partial decay of the ESA band, and essentially all the SE decays with a 2-ps lifetime (although a very weak 8-ps component is also observed). Similar behavior is observed in TMpCA at pH = 7 but with a slightly longer 3.7-ps lifetime.

In contrast to the neutral pH conditions, these chromophores show distinctly different dynamics at pH = 10.5. For TMpCA, the dynamics has been investigated in detail and presented elsewhere,[35,36] and the same data is reproduced here for

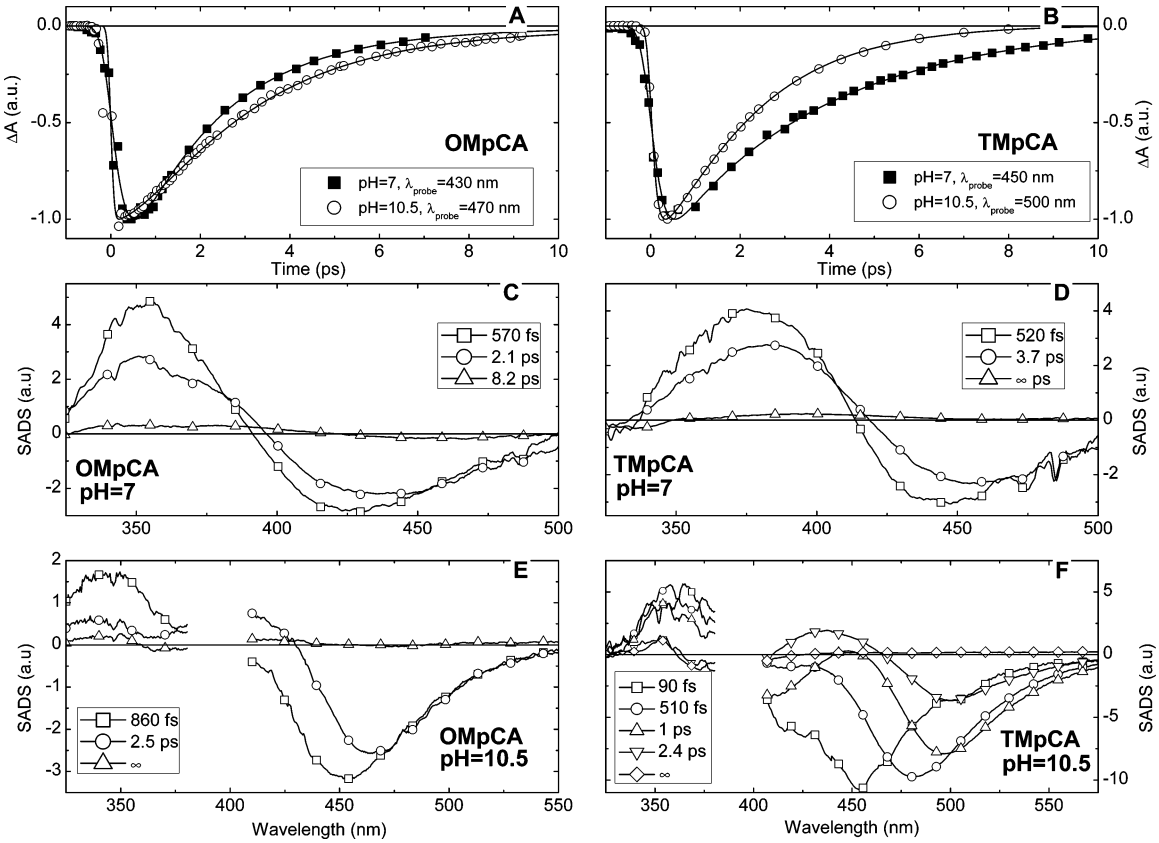

Figure 4. Time-resolved kinetic traces measured at the SE band of TMpCA (A) and OmpCA (B) at pH = 7 (squares) and 10.5 (circles) along with the global analysis fit to the data (solid lines). Excitation wavelength: 310 nm for pH = 7 and 395 nm for pH = 10. Probe wavelengths are shown in the legends. (C and E) SADS resulting from the sequential model fit to the data measured on OMpCA at pH = 7 and 10.5, respectively. (D and F) TMpCA SADS at pH = 7 and 10.5, respectively. The estimated time constants for the spectral evolution are shown in the legends.

comparison. Both pigments exhibit sharper and more asymmetric SE bands than pCA at all pH values and than their own counterparts at pH = 7. In both OMpCA and TMpCA, a significant red-shifting of the SE bands is observed at the time scale from 100 to 860 fs. In OMpCA, the resolution of the fast time scales is poorer than in TMpCA because of the smaller spectral overlap between the 395-nm excitation pulse and the ground-state absorption (parts C and D of Figure 1), which results in a greater contamination of the data with the cross-phase modulation artifact. The decay of SE is not significantly influenced by the pH (parts A and B of Figure 4). However, the most striking observation is that, along with the red-shifting and decay of SE, a rise of an IA band is observed peaking at ca. 390 nm for OMpCA (Figure 4E) and 440 nm for TMpCA (Figure 4F). The kinetic traces taken at the maximum of this IA band (not shown) exhibit similar features to those observed in the zero-crossing traces of pCA and SinFA at pH = 10.5 (parts A and C of Figure 2).

The pigments with methoxy group(s) attached to the phenolic ring (FerFA and SinFA) exhibit significantly longer lifetimes than pCA, TmpCA, and OMpCA; the traces at the peak of SE band of these pigments at different pH values are contrasted in Figure 5. Even though the excited-state decay is distinctly longer (~20 ps), the spectral features observed in the SADS are similar to those observed for the other pigments. A clear red-shift of the SE is observed in these chromophores that takes place from 600 to 2.8 ps, depending on the sample. Similar to pCA, in FerFA and SinFA at pH = 10.5 a decay of the IA band is observed along with a shift; this decay, however, is absent in the pH = 7 data, where the IA band remains unchanged during the first several ps (parts C and D of Figure 5). At pH = 7, the SE decay of both pigments is largely monoexponential and takes 19 ps in FerFA and 26 ps in SinFA. At pH = 10.5, two decay components are resolved in FerFA (8.2 and 44 ps); SinFA decay is largely monoexponential with an 18-ps lifetime. The SADS representing SE decay (44 ps for FerFA and 18 ps for SinFA) exhibit the most red-shifted SE band (parts E and F of Figure 5) and feature a shoulder on the red wing of the ESA band (ca. 425 nm). This spectral region was further investigated by PDP experiments (see below).

The FAL and TML chromophores, which have the C1−Cβ single bond and the Cα=Cβ double bond of their coumaryl tail locked, are essentially fluorescent dyes with a lifetime of the order of several nanoseconds (Figure 6). The SADS of both chromophores (parts B and C of Figure 6) show a dynamic red-shift of the SE with characteristic times of 320 fs and 2.2 ps in FAL and 200 fs and 1.27 ps in TML (the process with a lifetime shorter than our time resolution was also observed but is obscured by the cross-phase modulation artifact and not included in the graphs). In both compounds, clear monoexponential kinetic decays are observed, with time constants of 3.8 ns for FAL and 2.1 ns for TML.

In most of the chromophores, a weak component exhibiting no temporal dynamics in the time window of the experiment (4 ns) is observed. This "terminal spectrum", which is most noticeable in the SinFA dataset at pH = 10.5 (Figure 5F), exhibits a broad induced absorption band peaking to the red of our probe window (>650 nm) that is often accompanied by a narrower IA peak around or below 400 nm (parts C−F of Figure 5). These bands have been observed in TMpCA and other chromophores before[36,45] and are ascribed to the photoproducts arising from a two-photon ionization of the chromophore: solvated electrons (broad band peaking at 720 nm) and corresponding radicals (narrow induced absorption band).

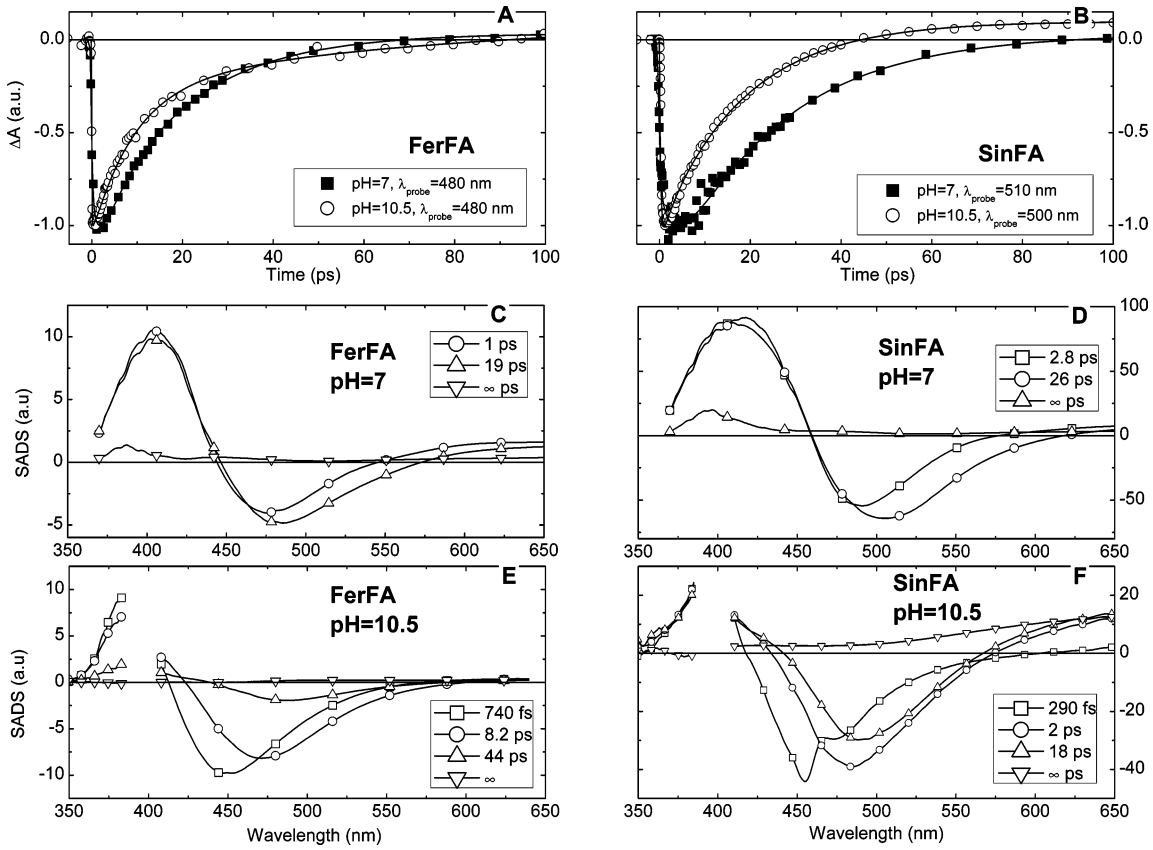

Figure 5. Time-resolved kinetic traces measured at the SE band of FerFA (A) and SinFA (B) at pH = 7 (filled squares) and pH = 10.5 (open circles) along with the global analysis fit to the data (solid lines). Excitation wavelength: 318 nm for the data measured at pH = 7 and 395 nm for pH = 10.5. Probe wavelengths are shown in the legends. (C and E) SADS resulting from the sequential model fit to the data measured on FerFA at pH = 7 and 10.5, respectively. (D and F) SinFA SADS at pH = 7 and 10.5, respectively. The estimated time constants for the spectral evolution are shown in the legends.

3.2. Excitation Wavelength Dependence. The observed dynamics in the pigments may be influenced by the amount of excess energy introduced into the molecule (i.e., they may depend on where in the absorption band the molecule is excited). For many of these chromophores, it is often impossible to select optimal wavelengths for excitation. The excess vibronic energy administered to the molecule is redistributed among the molecular vibrational degrees of freedom and subsequently transferred to the environment, and these processes may be reflected in the electronic transient spectra. In some cases, the absorption band of the pigment may be due to several closely spaced excited electronic states,[46] and the relaxation between those would depend on the initial populations created by the excitation pulse (in other words, the observed dynamics would also be sensitive to the excitation wavelength). To address this issue, dual-excitation PP experiments[47] were performed on FerFA and SinFA at pH = 10.5, at both 395 and 318 nm. While the low-energy excitation wavelength excites the far red edge of the absorption bands (see parts D and E of Figure 1) and little excess energy is delivered to the pigment, the high-energy 318-nm light excites the pigment in the high-energy wing of the ground-state absorption band and introduces 6500 cm^{-1} of additional excitation energy compared to the 395-nm pump pulses. Our setup allows us to perform the two PP experiments nearly simultaneously with ca. 10 ms time intervals between different pump pulses[47] so that the artifacts due to sample degradation or long-term laser stability are essentially excluded. The normalized PP traces taken at the IA and SE bands are contrasted in Figure 7. Essentially no difference is observed in photoinduced dynamics between the 318-nm excitation (circles and

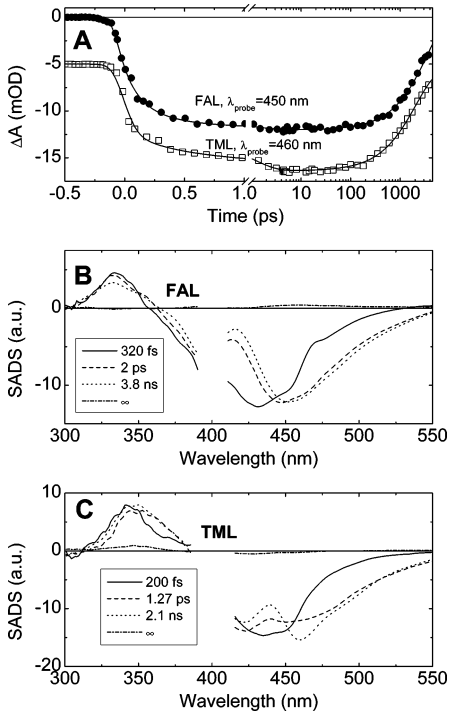

Figure 6. (A) Time-resolved kinetic traces measured at the SE band of FAL (closed circles) at 450 nm and TML (open squares) at 460 nm along with the global analysis fit to the data (solid lines). (B) Sequential SADS of FAL. (C) Sequential SADS of TML. The estimated time constants of the spectral evolution are shown in the legends.

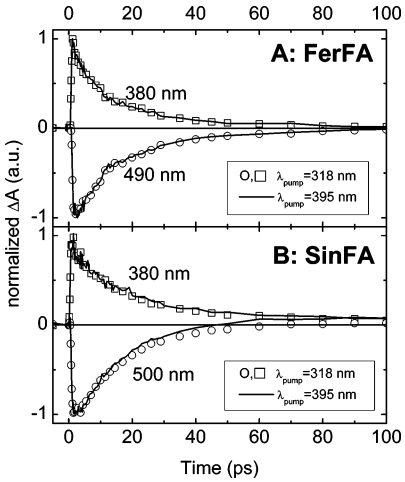

Figure 7. Normalized transient absorption traces measured on FerFA (A) and SinFA (B) with 318-nm (symbols) and 395-nm (solid lines) excitation. The probe wavelengths are indicated next to the curves.

squares) and 395-nm excitation (solid lines) for FerFA and SinFA. A small difference is observed in the SinFA data, where the SE appears to decay slightly faster for the 395-nm excitation case than the 318-nm case, but this effect can be ascribed to different terminal values, since the yield of two-photon ionization appears to be excitation wavelength dependent. This was confirmed by a global analysis fit to the data that revealed near-identical SADS and dynamics in the accessible time window (not shown). In the case of several near-degenerate states, one would expect an additional phase in the dynamics observed upon blue-wing excitation (which would reflect the relaxation between these states). Since the observed dynamics is nearly identical, it implies that either the relaxation among different vibrational substates (or, potentially, different electronic states) does not occur or that it is much faster than the time resolution of the experiment (370 fs in the case of 318-nm excitation) allows to detect.

3.3. PDP: SinFA vs TML and FAL. In the previous investigations on TMpCA, PDP spectroscopy was particularly insightful in characterizing and identifying overlapping bands in the measured PP spectra and elucidating underlying pathways of the photoinduced dynamics.[36,37,45,48] In TMpCA, the IA at the wavelengths between the GSB and SE was attributed to an unrealaxed ground state of the molecule.[36] Similar PDP experiments were performed here on SinFA, FAL, and TML at pH = 10.5 (excited using 395-nm light; the NOPA could be used to generate 505-nm dump pulses). The dump-induced effects on the PP signals are shown in Figure 8, where the PP signals measured in the SE and ESA bands (Figures 6 and 5F) as well as in the wavelength region between the GSB and SE are contrasted. The traces in Figure 8 represent double difference absorption signal (ΔΔOD), which is the difference between pump−probe signals with and without the presence of dump pulse[36]

$$\Delta\Delta\mathrm{OD}(\lambda,t_{\mathrm{probe}},t_{\mathrm{dump}}) = \mathrm{PDP}(\lambda,t_{\mathrm{probe}},t_{\mathrm{dump}}) - \mathrm{PP}(\lambda,t_{\mathrm{probe}}) - \mathrm{DP}(\lambda,t_{\mathrm{probe}} - t_{\mathrm{dump}}) \quad (1)$$

$\mathrm{PDP}(\lambda,t_{\mathrm{probe}},t_{\mathrm{dump}})$ denotes the PP signal with the dump pulse present, $\mathrm{PP}(\lambda,t_{\mathrm{probe}})$ is PP signal without the dump pulse (i.e., the "normal" PP signal), and $\mathrm{DP}(\lambda,t_{\mathrm{probe}} - t_{\mathrm{dump}})$ is a DP signal (i.e., pump pulse is off and dump pulse is present). In our case, where the wavelength of the dump pulse is nonresonant with the absorption of the sample, this signal accounts only for the scattering and cross-phase modulation due to the dump pulse.

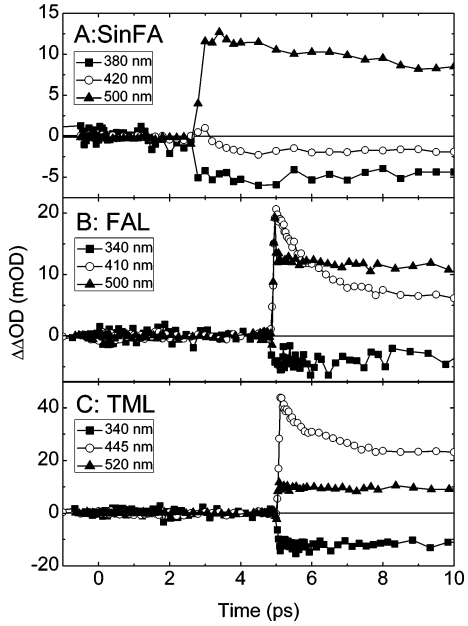

Figure 8. Dump-induced effect on the PP signals at the probe wavelengths corresponding to SE (solid triangles), ESA (solid squares) bands, and at the wavelengths between the GSB and SE band (hollow circles) in SinFA (A), FAL (B), and TML (C). The probe wavelengths are shown in the legends. Time zero is defined by the pump pulse, and the dump pulse arrives at ca. 2.8 ps in SinFA and ca. 5 ps in FAL and TML. The probe wavelengths are shown in the legends.

The data in Figure 8 show that both the SE and ESA bands are *instantaneously* diminished by the applied dump pulses (negative ΔΔOD signal indicates a decrease in PP signal and positive means increase), while at the wavelength between the GSB and SE (open circles), the dump effect exhibits a slower dynamics, with a lifetime of ca. 300 fs in SinFA and ca. 1.5 ps in FAL and TML. This dynamics is due to a short-lived unrelaxed ground state that is populated by the dump pulse.[36,45,49] When the molecule decays to the ground state via either fluorescence or internal conversion (processes much slower than the action of dump pulse), this short-lived ground-state intermediate never accumulates enough population to be observed directly in the PP experiment. However, for TMpCA and OMpCA at pH = 10.5, this species is clearly distinguishable in the PP signals alone, and the possible reasons for this are discussed below. As in similar phenolate-containing photoreceptor molecules, the terminal PP signals in these systems are unaffected by the presence and timing of the dump pulse (data not shown), which is expected for the combination of a hydrated electron and a radical, generated via a multiphoton mechanism.[36,37,45]

4. Discussion

It is clear from the absorption spectra in Figure 1, and the time-resolved data in the subsequent figures, that chromophore modifications and protonation state have a significant influence on the static and dynamic spectroscopic properties of these PYP model chromophores. In particular, the esterfied derivatives exhibit significantly red-shifted absorption spectra compared to the corresponding free acids (e.g., TMpCA and OMpCA vs pCA and TML vs. FAL); however, they are still blue-shifted compared to the absorption spectra of the same chromophores bound to the PYP apoprotein.[32] This is indicative of the special interactions between the protein environment and the embedded chromophore.[50] This esterfication-induced red-shifting is greatest when the phenolic moiety of the pigments is deprotonated (pH

= 10.5). In contrast to the esterfied chromophores, the pCA chromophore has three protonation states depending on whether the carboxylic acid or the phenolic moiety is protonated or both. It exhibits a peculiar dependence of the absorption spectrum on the protonation state. At pH = 2, the neutral form has its absorption maximum at 308 nm, and upon deprotonation of the carboxylic group (pH = 7), the peak of the spectrum shifts to the blue (285 nm); the deprotonation of the phenolic group at pH = 10.5 leads to an absorption spectrum that peaks further to the red than the neutral form (332 nm). In the other model chromophores, the deprotonated state at elevated pH always exhibits the more red-shifted absorption spectrum (Figure 1), which is a sign of the greater coupling of the charged chromophore to the solvent.

This sensitivity of the protonation state to the static properties of the chromophores indicates that the charge on the phenolic oxygen significantly alters the electron density distribution in the molecule and perhaps even affects the conjugation length. This has been suggested from previous Stark measurements of isolated PYP chromophores measured at different pH values[51] and from ab initio calculations on a model chromophore from the green fluorescent protein, which has a structure related to the PYP chromophores studied here.[52] In the locked pigments, a significant narrowing of the absorption spectra is observed compared to unlocked derivatives. One explanation for this may be the fact that, in these pigments, the ground-state distribution of torsional angles across the C1−Cα and the Cα=Cβ bonds cannot occur and does not contribute to the inhomogeneous broadening of the spectra. Alternatively, the electronic state structure of the chromophore (i.e., the bands due to closely spaced excited states) could have been partially modified by added bonds. In pCA, quantum calculations have predicted that multiple excited electronic states overlap, which gives rise to a broad absorption spectrum.[46,53] Levy and co-workers have observed effects of exciting into these states in the gas phase;[54] however, direct observation of these states in condensed phases and their influence in ensuing photochemistry has yet to be established.

4.1. Excited-State Dynamics. All the investigated chromophores exhibit a dynamic red-shift of the SE band on a time scale ranging from 200 fs (FAL and TML, Figure 6) to 2.8 ps (SinFA, Figure 5). Where time resolution allows its detection (e.g., 395-nm excitation datasets), the shifting dynamics is clearly multiexponential (Figure 6) with a sub-100-fs component and several slower phases extending to ca. 2 ps. In many of these chromophores, little or no decay of the emission is observed on these time scales (i.e., the amplitude of the SE band remains largely unchanged). In the previous studies of pCA at pH = 10.5, this spectral shift was not observed, possibly due to a poorer time resolution.[33,34] Both solvation dynamics and twisting are manifested as a dynamic red-shifting of fluorescence or SE bands.[10,55−57] A comparison of the dynamics observed in the locked vs free chromophores can be used to separate these effects.[35,38]

In a number of the investigated chromophores, a decay of the ESA band is observed on the same time scale (500 fs to 2 ps) as the solvation-induced SE shift (Figures 2−5). In contrast, the amplitude of the SE band does not decrease appreciably on these time scales. Such ESA decay cannot directly be attributed to solvation because the latter primarily manifests itself as a band shift rather than a change in the amplitude of the bands. Sometimes, solvation may account for amplitude changes in the spectral region where ESA and SE bands overlap, if the two bands shift differently upon solvation. However, the sub-picosecond decay of ESA is almost uniform across the whole ESA band and thus is probably caused by other processes. The observed decay of ESA could result from vibrational relaxation of the molecule. Different vibrational sublevels have different Franck−Condon factors that determine the transition probabilities. For harmonic oscillators, these factors are a function of the force constants (curvature of PESs) and the displacement of the potential minima on the vibrational coordinate.[58] It may be that, for our pigments, the maximum S_1-S_2 transition probability is achieved in a nonequilibrium population distribution among vibrational sublevels and hence vibrational relaxation in the S_1 state results in the decrease of ESA. Usually vibrational relaxation manifests itself as a narrowing of the SE and ESA bands[59] with a rate that is largely solvent independent.[60] However, the lack of excitation wavelength dependence of the PP data for SinFA and FerFA (Figure 7) indicates that vibrational relaxation (at least, the dynamics observable with our time resolution) does not appreciably affect the ESA dynamics in these pigments.

Another explanation of this peculiar behavior of the ESA vs SE might arise from different closely spaced electronic states that can be accessed by 310 nm excitation. Several near-degenerate states have been predicted for pCA in the protein environment by quantum-chemical calculations[46] and were indeed observed in gas-phase experiments.[54] When this mixture of different electronic states with different ESA and SE cross sections is excited, the relaxation between these states can give rise to a complex behavior of ESA and SE bands that may be similar to the one observed here. However, also in this case, a dependence on the excitation wavelength should be expected, because different excitation wavelengths would presumably excite different mixtures of electronic states which, in turn, would result in different relaxation dynamics. The observed absence of the excitation wavelength dependence implies that multiple electronic states responsible for the lowest absorption band of PYP, as predicted by quantum-chemical calculations,[46] either do not exist (i.e., there is only one electronic state responsible for the lowest-lying absorption band) or, more likely, interconvert into each other with a rate faster than our time resolution (370 fs in the case of 318-nm excitation) allows to detect. It must be noted though that the quantum-chemical calculations were made on the pigment different from the ones on which the excitation wavelength dependence was measured.

In comparison with the locked chromophores (TML and FAL), which remain in the excited state for several nanoseconds, all the studied chromophores exhibit dramatically shortened excited-state lifetimes (Table 1). This rapid quenching, which is typical of isomerizing chromophores,[10,61,62] is attributed to an enhanced internal conversion induced by the motion in the twisting coumaryl backbone of the chromophore.[33,63] Upon excitation, a rotation around a single or double bond, or a "hula twist",[64] occurs, which simultaneously decreases the S_1 energy and increases that of S_0, which leads to rapid internal conversion.[65] After relaxation to the ground state, the spatial configuration of the chromophore (and the solvent) is no longer in the minimum energy state and the system rearranges to relax into a lower energy configuration on the ground-state PES. Depending on the shape of the ground- and excited-state PESs, this process may result in the formation of the (meta)-stable isomers or a transient ground state species that quickly returns back to the original ground state (Figure 9). Often conical intersections (true intersecting electronic states) are involved in very fast (~1 ps) internal conversion rates[66] and may

TABLE 1: Summary of the Excited-State Lifetimes of the Studied Pigments[a]

pigment	pH	lifetime (ps)
pCA	2	2.6
	7	2.7
	10.5	9.4
TMpCA	7	3.7
	10.5	2
OMpCA	7	2.1
	10.5	2.5
FerFA	7	19
	10.5	8.2 (20% 44 ps)
SinFA	7	26
	10.5	18
FAL	10.5	3800
TML	10.5	2100

[a] The lifetime is defined as the inverse rate of the step in the evolutionary model (see Experimental Section), during which the largest fraction of stimulated emission is lost.

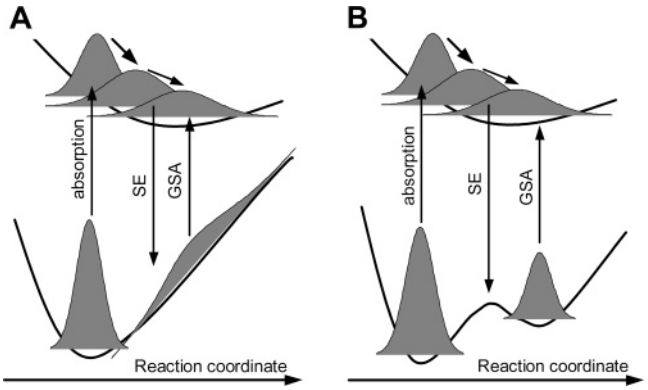

Figure 9. Model PESs along the twisting coordinate of the pigment. (A) Barrierless evolution in the ground state, resulting in the broad unrelaxed ground-state absorption; (B) evolution involving the ground-state barrier, resulting in the sharp ground-state absorption.

participate in the dynamics observed in the photoreceptors studied here.[67−69]

Apart from solvated electrons, no long-lived photoproducts (which could be attributed to the isomerized molecules) are observed in any of the chromophores studied, which means that the full trans−cis isomerization does not occur in the pigments in solution or occurs with a yield that is lower than our resolution allows us to detect (ca. 3%). The ultrafast quenching of the excited state results from the twisting reaction when the chromophore "attempts" to isomerize and twists in the excited state; however, after the intersystem crossing to the ground state, the shape of the PES is such that the molecule simply relaxes back to the original all-trans conformation (Figure 9A). For TmpCA, this behavior is fully consistent with the predictions based on quantum mechanical/molecular mechanics calculations by Groenhof et al.[67]

The unlocked chromophores without substitutions on the phenolic ring exhibit the lifetimes in the range between 2 and 3.7 ps, with the exception of pCA at pH = 10.5, which exhibits a 9.4-ps lifetime[33] (Table 1). A possible explanation as to why the excited-state lifetime is prolonged so much by the deprotonation of the phenolic oxygen in this particular pigment could be that it results in a different charge redistribution in the molecule upon excitation, and hence in a different excited-state pathway, the molecule follows after the excitation. Electro-optic measurements show that the magnitude of the charge displacement upon excitation of TMpCA and TML is significantly reduced when measured at neutral pH, where the phenolic moiety of the pigments is protonated.[51] If one assumes that the charge movement upon excitation is a crucial factor determining the isomerization pathway of the PYP chromophores, it becomes clear why, in the PYP protein system, the embedded chromophore is deprotonated (see below, section 4.3).

Among the unlocked and unsubstituted chromophores, only the pCA at pH=10.5 is doubly charged; other pigments have neutral ester groups on the coumaryl tail that are more likely to accommodate an electron density shifted from the phenolic oxygen. Indeed, the lifetime of pCA at pH = 10.5 is closer to that of FerFA and SinFA. Because the typical excited-state lifetimes observed for all the unsubstituted, unlocked model PYP chromophores are ∼2−3 ps and the excited-state lifetime for native PYP is ∼2 ps,[22,23] the pCA chromophore at pH = 10.5 is less relevant for understanding the excited-state dynamics of PYP.

The excited-state lifetime is also significantly longer in the pigments with the oxymethyl substitutions on the phenolic ring (FerFA and SinFA). It is tempting to ascribe this effect to the increased bulkiness of the phenolic end of the molecule, where, upon isomerization, the molecule would have to "drag along" a greater mass and experience a greater resistance from the solvent. However, because the carboxylic end of the molecule is much lighter than the phenolic ring (even without the oxymethyl substitutions), it is natural to assume that this end would preferentially move upon the twisting of the double bond in the coumaryl tail. These pigments are free acids and, similar to pCA, are doubly negatively charged at pH = 10.5. Their excited-state lifetime is also comparable to pCA at pH = 10.5, which provides a hint that it is not simply the "bulkiness" of the molecule but probably a more subtle change in the electronic structure and charge distribution of the pigment that affect the driving force (and hence the rate) for twisting. The pH dependence of the SE decay time in FerFA and SinFA is significantly weaker than (and opposite to) the one observed in the bare pCA chromophore; the pigments with a charged phenolic oxygen exhibit a slightly faster decay than singly charged ones (parts A and B of Figure 5). The oxymethyl groups are charge donor groups and should affect the dipole moment of the pigment in the ground and excited states, which would, in turn, affect the twisting time scales through the solvent by enlarging or reducing the number of coordinated solvent molecules and thus increasing or reducing the friction for twisting. Preliminary experiments exploring the dependence of SE decay times on the viscosity of the solvent (data not shown) have confirmed that increasing the viscosity does slow the excited-state lifetime.

The characterization of the PESs involved is an important component in understanding the photophysics underlying the photoinduced twisting reactions, because these surfaces ultimately determine the driving force for the excited- and ground-state evolution. An intriguing question about the model PYP chromophore is whether an energy barrier is hindering the excited-state twisting process. This has been discussed extensively for the isomerization of the chromophore in bacteriorhodopsin,[48,61,70,71] where a three-state model, which includes a small excited-state energy barrier, was favored over a two-state barrierless model. The dual-excitation wavelength PP experiment provides evidence that no significant energy barrier exists for twisting in the excited state for the FerFA and SinFA pigments: the observed quenching dynamics is identical regardless of the excitation wavelength (310 nm vs 395 nm). If the excess energy of 310-nm excitation contributed to crossing an excited-state barrier, the observed twisting would be faster and/or occur with a higher yield than using a more red excitation

wavelength, which is obviously not the case. In contrast, for PYP, an excited-state energy barrier was proposed to explain both steady-state[72,73] and ultrafast experiments.[38] It must be noted though that the pigments studied with dual PP spectroscopy (FerFA and SinFA at pH = 10.5) exhibit relatively long excited-state quenching times compared to those of solvation and/or vibrational relaxation. Similar experiment on TMpCA (currently planned), where the twisting rate is much faster and commensurate with the solvation/vibrational relaxation time scales, would allow us to establish whether the twisting time scales of this pigment in solution are sensitive to the excitation wavelength, in other words, whether it involves an excited-state energy barrier as predicted by Groenhof et al.[74]

4.2. Ground-State Dynamics. In TMpCA and OMpCA at pH = 10.5, an IA band between the GSB and SE bands (parts E and F of Figure 4) is clearly observed with a delay after the excitation. For TMpCA at pH = 10.5, this band has been studied in detail with PDP spectroscopy and was attributed to a structurally unrelaxed ground-state intermediate of the pigment.[63] Moreover, a similar ground-state intermediate has been shown to occur in PYP as well, which highlights the similarity of dynamics of TMpCA and PYP.[37] A similar band was also observed in another PYP model chromophore containing a thiophenyl group,[34] the chromophore of the green fluorescent protein, (with a similar conjugated π-electron system as the pigments investigated here) and several molecules that undergo twisting-induced charge-transfer reactions.[45,75] This, along with the fact that this band is observed in OMpCA as well (albeit slightly obscured by the pump scatter at 395 nm, Figure 4E), indicates that the observation of this band is not unique to the presence of the thioester group.

The PDP results on SinFA, TML, and FAL (Figure 8) show that an unequilibrated ground-state species is also observed in these pigments, but it is much less pronounced than in TMpCA. In SinFA, instead of a clearly separated IA band, it manifests itself in pump−probe signals as a shoulder in the red part of the ESA band (18-ps SADS in Figure 5F). The late excited-state SADS of many other pigments exhibit a similar feature (Figures 3 (parts B and D), 4 (parts C and D), and 5 (parts E and F)) which is the manifestation of ground-state intermediates. In all these pigments, the transients taken around the zero-crossing points of the spectra show similar behavior to that observed in pCA at pH = 10.5 (Figure 2B), where at early times the PP signal is dominated by the SE, and as the latter shifts to the red due to solvation (and perhaps twisting), the ground-state intermediate absorption rises and then decays.

The unrelaxed ground state is also present in the locked pigments, which have much longer excited-state lifetimes and cannot twist, although here it is completely masked by the excited-state spectral features, and only PDP experiments can clearly uncover it (parts B and C of Figure 8). The fact that the pigments without rotational degrees of freedom also feature this ground-state species indicates that it is not a unique signature of a twisting reaction and must result from other processes such as ground-state solvation and/or vibrational relaxation.[36] When the pigments are dumped from the excited state, their dipole moment and polarizability changes; the configuration of the surrounding solvent molecules, adjusted to accommodate the excited state pigment, no longer corresponds to the energetic minimum. The molecule might also be dumped into a vibrationally excited ground state and have some excess vibrational energy that needs to be dissipated in the solvent. Thus, after dumping, the reaction akin to the excited-state solvation or vibrational relaxation will take place in the ground state.[76] Such phenomena occur on <2-ps time scales, similar to the ones observed here, and are responsible for the dynamics observed in FAL and TML.

The fact is that the unrelaxed ground-state species is so pronounced (with well-defined separate spectral band with its own dynamics) in TMpCA and OMpCA at pH = 10.5 but is difficult to detect (a slight shoulder in the excited-state spectrum) in other pigments deserves comment. Even in TMpCA and OMpCA at neutral pH, only hints (the shoulder on the red part of the ESA band) for the formation of this species are observed. SinFA and FerFA show a similar shoulder in the spectrum at pH = 10.5 (parts E and F of Figure 5) but not at pH = 7 (parts C and D of Figure 5). Several factors may influence the intensity of this feature: (1) in some cases, the lifetime of the unrelaxed ground state can be quite short (compared to the lifetime of the excited state), and the population of this state is never enough to be able to observe it in PP signals; (2) its transition dipole is weak, and its induced absorption is dominated by other overlapping bands; (3) the ground-state absorption will be dominated by the SE and ESA bands. The first two factors can play a role *only* if the observed ground-state intermediate is due to an inherent structural rearrangement of the molecule; because solvation/vibrational relaxation time scales do not strongly depend on the solute, neither do these processes affect the transition dipole moment of the pigments. At the same time, the excited-state lifetimes of TMpCA and OMpCA at pH = 7 are not significantly different from those at pH = 10.5 (Table 1), suggesting that the same amount of this ground-state intermediate would be formed, if it was due to the ground-state solvation or vibrational relaxation. This allows us to conclude that the observed ground-state band and its dynamics in TMpCA and OMpCA at pH = 10.5 are the result of a specific pathway (only occurring in these pigments) in the excited-state relaxation, whereas in other pigments (including the locked ones), the observed spectral features are ascribed to ground-state solvation/vibrational relaxation.

In the case of a structural reorganization, the precise dynamics will be a function of the ground- and excited-state PES along the twisting coordinate (Figure 9). The lifetime of the ground-state intermediate is directly governed by the slope of the ground-state PES (the driving force for the return to the equilibrated ground state). To a first approximation, the transition dipole at a given point on the PES should be the same for the IA and SE; however, depending on the shape of the PES, the population distributions can be different. For example, if the ground-state PES has a local minimum, a significant amount of the population will be localized there for some time and when projected on an excited state PES, will give a rise to a more-defined band (Figure 9B). However, if the ground-state potential is shallow and monotonic, a broad distribution of the population will occur and the resulting IA will be a relatively featureless broad band that is easily masked by other spectral features (Figure 9A). Because PDP spectroscopy, particularly in combination with global analysis,[36,37,45] simultaneously explores both the ground- and excited-state dynamics, the corresponding PES can be reconstructed from the data.[75]

4.3. Relationship to PYP. The photocycle dynamics of PYP has the most in common with the OMpCA and TMpCA chromophores at pH = 10.5.[21,24,37] These systems have similar properties: (a) an ester group (thio- or oxymethyl) instead of a negatively charged carboxylic oxygen on the coumaryl tail; (b) deprotonated phenolic groups;[77,78] (c) fast excited-state quenching due to twisting and/or isomerization; and (d) pronounced unequilibrated ground-state species featuring IA at the wave-

lengths between the GSB and SE.[35,36] These features are observed only with the phenolic moiety deprotonated (high pH), while at neutral pH, their dynamics is comparable with the other model chromophores. This strong dependence on the protonation state indicates that a charge (re)distribution in the molecule is the key factor that determines the dynamics of the pigment. This has also been proposed by recent electro-optic experiments on TMpCA, which showed a large (25 D) dipole moment difference between the ground and excited state, making TMpCA essentially a charge-transfer molecule at high pH,[51] while at the same time, the neutral form of TMpCA exhibits a much smaller (9 D) charge displacement.[51] Unfortunately, the dipole moment change in OMpCA has not been measured. The charge displacement effect is also noticeable on the ultrafast dynamics of pCA: the quenching lifetime here changes from 2.6 ps and neutral and acidic pH to 9.4 ps at basic pH; however, the spectral features in this pigment of the excited (and, possibly, ground) states are altered only slightly by the protonation. Similarly long lifetimes at high pH are observed in other doubly charged pigments: SinFA and FerFA at pH = 10.5. In these compounds that feature bulky (and electron-donating) groups on the phenolic ring, the protonation effect is less obvious, most probably because the electron density can be borrowed from *both* the oxymethyl groups and the phenolic oxygen and the charge stabilization on the phenolic oxygen by the proton becomes less important. Ab initio calculations to verify this are currently in progress.

To summarize, from the experimental observations, one can infer that the PES for twisting is significantly altered by removing the charge from the coumaryl tail of the pigment and replacing it with ester groups (OMpCA and TMpCA). The strong pH dependence of the excited-state dynamics and the recent Stark experiments[51] suggest that the twisting is probably stabilized, or even funneled, by the solvent (or protein) environment that reacts to the large change in dipole moment upon excitation that is characteristic to these particular chromophores. The short excited-state lifetimes of all nonlocked pigments suggest that *all* of them twist thereby dissipating the excitation energy, but only TMpCA and OMpCA at pH = 10.5 *twist differently*, resulting in an unequilibrated ground state also observed in PYP.[36,37] Perhaps the same twisting pathway leads to the initiation of PYP photocycle: the photocycle is initiated as a response of the protein to the changed dipole moment *which affects* the twisting of the chromophore. The hints on the precise mechanism of such a response are offered by the recent visible pump−IR probe experiments on wild-type PYP and the mutants, which showed that the hydrogen bond between the phenolate oxygen of the chromophore and glutamate-46 residue in the protein was instantaneously weakened upon excitation, presumably due to a charge redistribution on the pigment.[79] Such a change in the hydrogen bonding network around the pigment can then provide a "feedback" for the excited-state dynamics, i.e., funnel the excited-state twisting of the chromophore, ultimately resulting in the later photocycle intermediates. This hypothesis is also in line with recent visible PP and PDP experiments that have shown that, in PYP, the efficiency of initiating the photocycle decreases with time.[25,37] If the mentioned protein response to the dipole change in the pigment is of concerted (coherent) nature, this should be expected, because as the time passes the vibrational coherence is lost and the probability of entering the photocycle decreases.

Additional Stark experiments on these model PYP chromophores at different protonation states should allow researchers to check whether the correlation between the observed ground state and the dipole moment change holds in more cases than TMpCA. Also, a study on the different chromophores (both in solution and in the protein) that have the rotation of the phenolic ring locked (with the double bond free) might be insightful.

5. Conclusions

We have investigated the ultrafast dynamics of a number of model PYP chromophores. Comparison of the free chromophores with the locked chromophores allowed us to attribute the red-shift of the SE band, occurring on the time scales of 100 fs to 2 ps, to predominately solvation dynamics, while isomerization manifested itself primarily as the quenching of stimulated emission.[38] A transient ground-state intermediate, resulting from unsuccessful "attempts" to isomerize can be directly observed in PP data for TMpCA and OMpCA at pH = 10.5. A similar intermediate has been revealed in SinFA, FAL, and TML by the use of PDP spectroscopy. However, in these pigments, it is attributed entirely due to ground-state solvation and/or vibrational relaxation. Spectral features in the PP spectra of other pigments suggest that it exists there as well. We suggest that in TMpCA and OMpCA the ground-state intermediate reflects the different pathway of structural evolution in excited and ground states. The prerequisite for it is the ester group (thiomethyl or oxymethyl) on the coumaryl tail of the pigment and the negative charge on the phenolic oxygen. These two features presumably enhance the charge-transfer character of the $S_0 \rightarrow S_1$ transition which, through the interaction with the environment, alters the course of twisting in these pigments. A similar interaction with the environment may be responsible for the photocycle initiation in PYP.

Acknowledgment. M.V. is grateful to The Netherlands Organization of Fundamental Research of Matter; D.S.L. would like to thank the Human Frontier Science Program Organization for providing financial support with a long-term fellowship.

References and Notes

(1) Feringa, B. L.; van Delden, R. A.; Koumura, N.; Geertsema, E. M. *Chem. Rev.* **2000**, *100*, 1789.
(2) Hampp, N. *Chem. Rev.* **2000**, *100*, 1755.
(3) Irie, M. *Chem. Rev.* **2000**, *100*, 1685.
(4) Kochendoerfer, G. G.; Mathies, R. A. *Isr. J. Chem.* **1995**, *35*, 211.
(5) Oesterhelt, D.; Stoeckenius, W. *Nat. New Biol.* **1971**, *233*, 149.
(6) Kennis, J. T. M.; Crosson, S.; Gauden, M.; van Stokkum, I. H. M.; Moffat, K.; van Grondelle, R. *Biochemistry* **2003**, *42*, 3385.
(7) Hellingwerf, K. J.; Hendriks, J.; Gensch, T. *J. Phys. Chem. A* **2003**, *107*, 1082.
(8) Sumitani, M.; Nakashima, N.; Yoshihara, K.; Nagakura, S. *Chem. Phys. Lett.* **1977**, *51*, 183.
(9) Glasbeek, M.; Zhang, H. *Chem. Rev.* **2004**, *104*, 1929.
(10) Hamm, P.; Zurek, M.; Röschinger, T.; Patselt, H.; Oesterhelt, D.; Zinth, W. *Chem. Phys. Lett.* **1996**, *263*, 613.
(11) Meyer, T. E. *Biochim. Biophys. Acta* **1985**, *806*, 175.
(12) Sprenger, W. W.; Hoff, W. D.; Armitage, J. P.; Hellingwerf, K. J. *J. Bacteriol.* **1993**, *175*, 3096.
(13) Borgstahl, G. E.; Williams, D. R.; Getzoff, E. D. *Biochemistry* **1995**, *34*, 6278.
(14) Genick, U. K.; Borgstahl, G. E.; Ng, K.; Ren, Z.; Pradervand, C.; Burke, P. M.; Srajer, V.; Teng, T. Y.; Schildkamp, W.; McRee, D. E.; Moffat, K.; Getzoff, E. D. *Science* **1997**, *275*, 1471.
(15) Genick, U. K.; Devanathan, S.; Meyer, T. E.; Canestrelli, I. L.; Williams, E.; Cusanovich, M. A.; Tollin, G.; Getzoff, E. D. *Biochemistry* **1997**, *36*, 8.
(16) Genick, U. K.; Soltis, S. M.; Kuhn, P.; Canestrelli, I. L.; Getzoff, E. D. *Nature* **1998**, *392*, 206.
(17) Hoff, W. D.; Dux, P.; Hard, K.; Devreese, B.; Nugteren-Roodzant, I. M.; Crielaard, W.; Boelens, R.; Kaptein, R.; van Beeumen, J.; Hellingwerf, K. J. *Biochemistry* **1994**, *33*, 13959.
(18) Xie, A.; Kelemen, L.; Hendriks, J.; White, B. J.; Hellingwerf, K. J.; Hoff, W. D. *Biochemistry* **2001**, *40*, 1510.
(19) van Brederode, M. E.; Hoff, W. D.; Van Stokkum, I. H.; Groot, M. L.; Hellingwerf, K. J. *Biophys. J.* **1996**, *71*, 365.

(20) Meyer, T. E.; Tollin, G.; Causgrove, P.; Cheng, P.; Blankenship, R. E. *Biophys. J.* **1991**, *59*, 988.
(21) Baltuška, A.; van Stokkum, I. H. M.; Kroon, A.; Monshouwer, R.; Hellingwerf, K. J.; van Grondelle, R. *Chem. Phys. Lett.* **1997**, *270*, 263.
(22) Changenet, P.; Zhang, H.; van der Meer, M. J.; Hellingwerf, K. J.; Glasbeek, M. *Chem. Phys. Lett.* **1998**, *282*, 276.
(23) Chosrowjan, H.; Mataga, N.; Nakashima, N.; Imamoto, Y.; Tokunaga, F. *Chem. Phys. Lett.* **1997**, *270*, 267.
(24) Devanathan, S.; Pacheco, A.; Ujj, L.; Cusanovich, M.; Tollin, G.; Lin, S.; Woodbury, N. *Biophys. J.* **1999**, *77*, 1017.
(25) Gensch, T.; Gradinaru, C. C.; van Stokkum, I. H. M.; Hendriks, J.; Hellingwerf, K.; van Grondelle, R. *Chem. Phys. Lett.* **2002**, *356*, 347.
(26) Chosrowjan, H.; Mataga, N.; Shibata, Y.; Imamoto, Y.; Tokunaga, F. *J. Phys. Chem. B* **1998**, *102*, 7695.
(27) Mataga, N.; Chosrowjan, H.; Shibata, Y.; Imamoto, Y.; Tokunaga, F.; Tanaka, F. *J. Lumin.* **2000**, *87*−*9*, 821.
(28) Mataga, N.; Chosrowjan, H.; Taniguchi, S.; Hamada, N.; Tokunaga, F.; Imamoto, Y.; Kataoka, M. *Phys. Chem. Chem. Phys.* **2003**, *5*, 2454.
(29) Mataga, N.; Chosrowjan, H.; Shibata, Y.; Imamoto, Y.; Kataoka, M.; Tokunaga, F. *Chem. Phys. Lett.* **2002**, *352*, 220.
(30) Hanada, H.; Kanematsu, Y.; Kinoshita, S.; Kumauchi, M.; Sasaki, J.; Tokunaga, F. *J. Lumin.* **2001**, *94*, 593.
(31) Cordfunke, R.; Kort, R.; Pierik, A.; Gobets, B.; Koomen, G. J.; Verhoeven, J. W.; Hellingwerf, K. J. *Proc. Natl. Acad. Sci. U.S.A.* **1998**, *95*, 7396.
(32) van der Horst, M. Structure/function relations in Photoactive Yellow Protein. Ph.D. Thesis, University of Amsterdam, 2004.
(33) Changenet-Barret, P.; Plaza, P.; Martin, M. M. *Chem. Phys. Lett.* **2001**, *336*, 439.
(34) Changenet-Barret, P.; Espagne, A.; Katsonis, N.; Charier, S.; Baudin, J.-B.; Jullien, L.; Plaza, P.; Martin, M. M. *Chem. Phys. Lett.* **2002**, *365*, 285.
(35) Larsen, D. S.; Vengris, M.; van Stokkum, I. H. M.; van der Horst, M.; Cordfunke, R.; Hellingwerf, K. J.; van Grondelle, R. *Chem. Phys. Lett.* **2003**, *369*, 563.
(36) Larsen, D. S.; Vengris, M.; van Stokkum, I. H. M.; van der Horst, M.; de Weerd, F. L.; Hellingwerf, K. J.; van Grondelle, R. *Biophys. J.* **2004**, *86*, 2538.
(37) Larsen, D. S.; van Stokkum, I. H. M.; Vengris, M.; van der Horst, M.; Hellingwerf, K.; van Grondelle, R. *Biophys. J.* **2004**, *87*, 1858.
(38) Vengris, M.; van der Horst, M.; Zgrablic, G.; van Stokkum, I. H. M.; Haacke, S.; Chergui, M.; Hellingwerf, K. J.; van Grondelle, R.; Larsen, D. S. *Biophys. J.* **2004**, *87*, 1848.
(39) Gradinaru, C. C.; van Stokkum, I. H. M.; Pascal, A. A.; van Grondelle, R.; van Amerongen, H. *J. Phys. Chem. B* **2000**, *104*, 9330.
(40) Hoff, W. D.; van Stokkum, I. H. M.; van Ramesdonk, H. J.; van Brederode, M. E.; Brouwer, A. M.; Fitch, J. C.; Meyer, T. E.; van Grondelle, R.; Hellingwerf, K. J. *Biophys. J.* **1994**, *67*, 1691.
(41) Holzwarth, A. R. Data Analysis in time-resolved measurements. In *Biophysical Techniques in Photosynthesis*; Amesz, J., Hoff, A. J., Eds.; Kluwer: Dordrecht, The Netherlands, 1996.
(42) van Stokkum, I. H. M.; Larsen, D. S.; van Grondelle, R. *Biochim. Biophys. Acta* **2004**, *1657*, 82.
(43) Ekvall, K.; van der Meulen, P.; Dhollande, C.; Berg, L. E.; Pommeret, S.; Naskrecki, R.; Mialocq, J. C. *J. Appl. Phys.* **2000**, *87*, 2340.
(44) Kovalenko, S. A.; Dobryakov, A. L.; Ruthmann, J.; Ernsting, N. P. *Phys. Rev. A* **1999**, *59*, 2369.
(45) Vengris, M.; van Stokkum, I. H. M.; He, X.; Bell, A.; Tonge, P. J.; van Grondelle, R.; Larsen, D. S. *J. Phys. Chem. A* **2004**, *108*, 4587.
(46) Molina, V.; Merchan, M. *Proc. Natl. Acad. Sci. U.S.A.* **2001**, *98*, 4299.
(47) Larsen, D. S.; Papagiannakis, E.; van Stokkum, I. H. M.; Vengris, M.; Kennis, J. T. M.; van Grondelle, R. *Chem. Phys. Lett.* **2003**, *381*, 733.
(48) Gai, F.; McDonald, J. C.; Anfinrud, P. *J. Am. Chem. Soc.* **1997**, *119*, 6201.
(49) Papagiannakis, E.; Larsen, D. S.; van Stokkum, I. H. M.; Vengris, M.; Hiller, R. G.; van Grondelle, R. In preparation.
(50) Yoda, M.; Houjou, H.; Inoue, Y.; Sakurai, M. *J. Phys. Chem. B* **2001**, *105*, 9887.
(51) Premvardhan, L. L.; Buda, F.; van der Horst, M. A.; Luehrs, D.; Hellingwerf, K. J.; van Grondelle, R. *J. Phys. Chem. B* **2004**, *108*, 5138.
(52) Voityuk, A. A.; Kummer, A. D.; Michel-Beyerle, M. E.; Rosch, N. *Chem. Phys.* **2001**, *269*, 83.
(53) He, Z.; Martin, C. H.; Birge, R.; Freed, K. F. *J. Phys. Chem. A* **2000**, *104*, 2939.
(54) Ryan, W.; Gordon, D. J.; Levy, D. H. *J. Am. Chem. Soc.* **2002**, *124*, 6194.
(55) Jimenez, R.; Fleming, G. R.; Kumar, P. V.; Maroncelli, M. *Nature* **1994**, *369*, 471.
(56) Jordanides, X. J.; Lang, M. J.; Song, X. Y.; Fleming, G. R. *J. Phys. Chem. B* **1999**, *103*, 7995.
(57) Kovalenko, S. A.; Ruthmann, J.; Ernsting, N. P. *Chem. Phys. Lett.* **1997**, *271*, 40.
(58) van Amerongen, H.; Valkunas, L.; van Grondelle, R. *Photosynthetic Excitons*; World Scientific: Singapore, 2000.
(59) Zgrablic, G.; Vo_tchovsky, K.; Kindermann, M.; Chergui, M.; Haacke, S. Ultrafast photophysics of the protonated Schiff base of retinal in alcohols studied by femtosecond fluorescence up-conversion. In *Femtochemistry and Femtobiology: Ultrafast Events in Molecular Science*; Martin, M. M., Hynes, J. T., Eds.; Elsevier: Paris, 2003.
(60) Zhang, J. P.; Chen, C. H.; Koyama, Y.; Nagae, H. *J. Phys. Chem. B* **1998**, *102*, 1632.
(61) Gai, F.; Hasson, K. C.; McDonald, J. C.; Anfinrud, P. A. *Science* **1998**, *279*, 1886.
(62) Waldeck, D. H. *Chem. Rev.* **1991**, *91*, 415.
(63) Larsen, D. S.; Vengris, M.; van Stokkum, I. H. M.; van der Horst, M.; Hellingwerf, K.; van Grondelle, R. *Biophys. J.* **2004**.
(64) Liu, R. S. H.; Hammond, G. S. *Proc. Natl. Acad. Sci. U.S.A.* **2000**, *97*, 11153.
(65) Fain, B. *Irreversibilities in quantum mechanics*; Kluwer Academic Publishers: Dordrecht, Boston, London, 2000.
(66) Domcke, W.; Stock, G. *Adv. Chem. Phys.* **1997**, *1001*, 1.
(67) Groenhof, G.; Bouxin-Cademartory, M.; Hess, B.; de Visser, S.; Brendendsen, H.; Olivucci, M.; Mark, A. E.; Robb, M. A. *J. Am. Chem. Soc.* **2004**, *126*, 4228.
(68) Toniolo, A.; Olsen, S.; Manohar, L.; Martinez, T. J. *Faraday Discuss.* **2004**, *127*, 149.
(69) Ko, C.; Levine, B.; Toniolo, A.; Monohar, L.; Olsen, S.; Werner, H.-J.; Martínez, T. J. *J. Am. Chem. Soc.* **2003**, *125*, 12710.
(70) Gonzalez-Luque, R.; Garavelli, M.; Bernardi, F.; Merchan, M.; Robb, M. A.; Olivucci, M. *Proc. Natl. Acad. Sci. U.S.A.* **2000**, *97*, 9379.
(71) Humphrey, W.; Lu, H.; Logunov, I.; Werner, H. J.; Schulten, K. *Biophys. J.* **1998**, *75*, 1689.
(72) Hoff, W. D.; Kwa, S. L. S.; van Grondelle, R.; Hellingwerf, K. J. *Photochem. Photobiol.* **1992**, *56*, 529.
(73) van der Horst, M. A. Unpublished results, 2004.
(74) Groenhof, G.; Bouxin-Cademartory, M.; Hess, B.; De Visser, S. P.; Berendsen, H. J. C.; Olivucci, M.; Mark, A. E.; Robb, M. A. *J. Am. Chem. Soc.* **2004**, *126*, 4228.
(75) Abramavicius, D.; Gulbinas, V.; Valkunas, L.; Shiu, Y.-J.; Liang, K.; Hayashi, M.; Lin, S. *J. Phys. Chem. A* **2002**, *106*, 8864.
(76) Changenet-Barret, P.; Choma, C.; Gooding, E.; DeGrado, W.; Hochstrasser, R. M. *J. Phys. Chem. B* **2000**, *104*, 9322.
(77) Cusanovich, M. A.; Meyer, T. E. *Biochemistry* **2003**, *42*, 4759.
(78) Kort, R.; Phillips-Jones, M. K.; van Aalten, D. M.; Haker, A.; Hoffer, S. M.; Hellingwerf, K. J.; Crielaard, W. *Biochim. Biophys. Acta* **1998**, *1385*, 1.
(79) Groot, M. L.; van Wilderen, L.; Larsen, D. S.; van der Horst, M. A.; van Stokkum, I. H. M.; Hellingwerf, K. J.; van Grondelle, R. *Biochemistry* **2003**, *42*, 10054.